

Untwisting the Boerdijk–Coxeter Helix

Robert L. Read read.robert@gmail.com

Abstract. The Boerdijk–Coxeter helix (BC helix, or tetrahelix) is a face-to-face stack of regular tetrahedra forming a helical column. Considering the edges of these tetrahedra as structural members, the resulting structure is attractive and inherently rigid, and therefore interesting to architects, mechanical engineers, and robotocists. A formula is developed that matches the visually apparent helices forming the outer rails of the BC helix. This formula is generalized to a formula convenient to designers. Formulae for computing the parameters that give edge-length minimax-optimal tetrahelices are given, defining a continuum of tetrahelices of varying curvature. The endpoints of the optimality of this continuum are the BC helix and a structure of zero curvature, the *equitetrabeam*. Numerically finding the rail angle from the equation for pitch allows optimal tetrahelices of any pitch to be designed. An interactive tool for such design and experimentation is provided: <https://pubinv.github.io/tetrahelix/>. A formula for the inradius of optimal tetrahelices is given. Utility for static and variable geometry truss/space frame design and robotics is discussed.

Key words. Boedijk–Coxeter helix, tetrahelix, robotics, tetrobot, unconventional robots, structural engineering, mechanical engineering, tensegrity, variable-geometry truss

18 AMS subject classifications. 51M15

1. Introduction. The Boerdijk–Coxeter helix[3] (BC helix), is a face-to-face stack of tetrahedra that winds about a straight axis. Because architects, structural engineers, and robotics are inspired by and follow such regular mathematical models but can also build structures and machines of differing or even dynamically changing length, it is useful to develop the mathematics of structures formed from tetrahedra where we relax regularity.

The vertices of the tetrahedra lie upon three helices about the central axis. The Glussbot[11] (or Tetrobot)[8] uses the regularity of this geometry to make a tentacle-like robot that can crawl like a slug or mollusc. These modular robot systems uses mechanical actuators which can change their length, connected by special joints, such as the 3D printable Song-Kwon-Kim[15] joint in the case of the Glussbot, or the CMS joint[7], in the case of the Tetrobot, which allow many members to meet in a single point. Such machines can follow purely regular mathematical models such as the Boerdijk-Coxeter helix or the Octet Truss[4].

31 Buckminster Fuller called the BC helix a *tetrahelix*[5], a term now commonly used. In
 32 this paper we reserve *BC helix* to mean the purely regular structure and use *tetrahelix* to refer
 33 to any structure isomorphic to the BC helix.

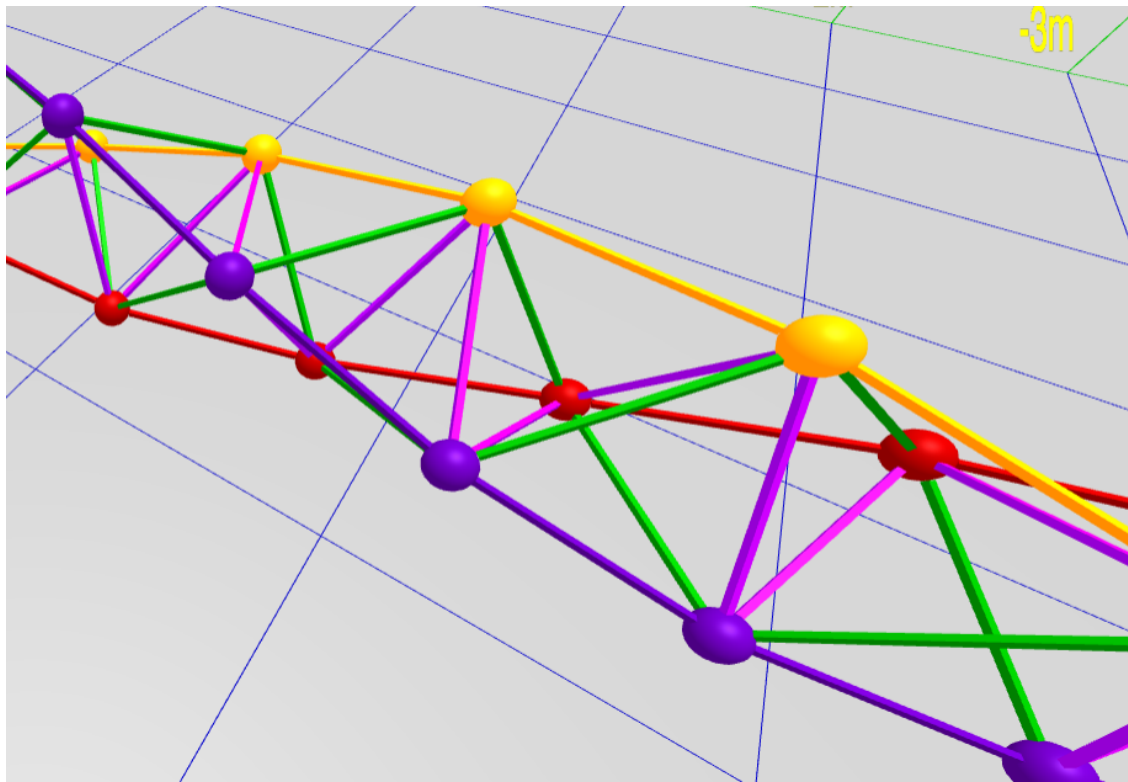


Figure 1. BC Helix Close-up (partly along axis)

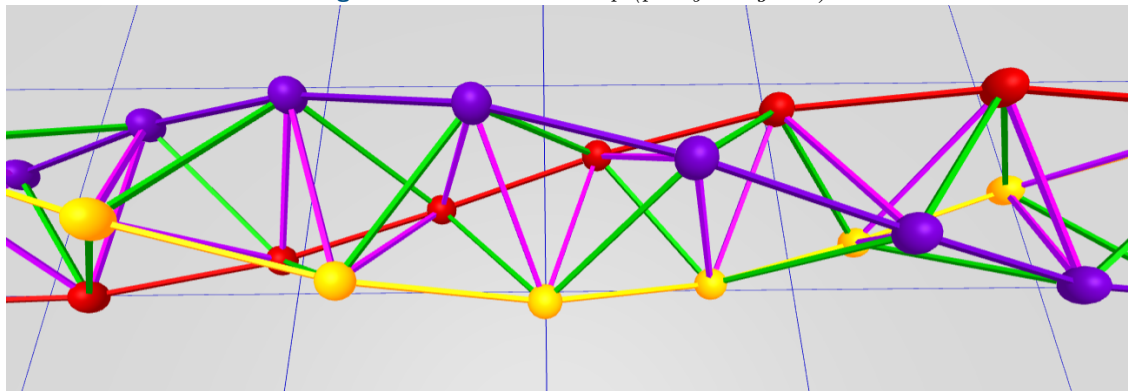


Figure 2. BC Helix Close-up (orthogonal)

34 Imagining Figure 2 as a static mechanical structure, we observe that it is useful to the
 35 mechanical engineer or robotocist because the structure remains an inherently rigid, omni-
 36 triangulated space frame, which is mechanically strong. Imagine further in Figure 2, that each
 37 static edge was replaced with an actuator that could dynamically become shorter or longer in
 38 response to electronic control, and the vertices were a joint that supported sufficient angular
 39 displacement for this to be possible. An example of such a machine is a glussbot, shown in
 40 Figure 11.

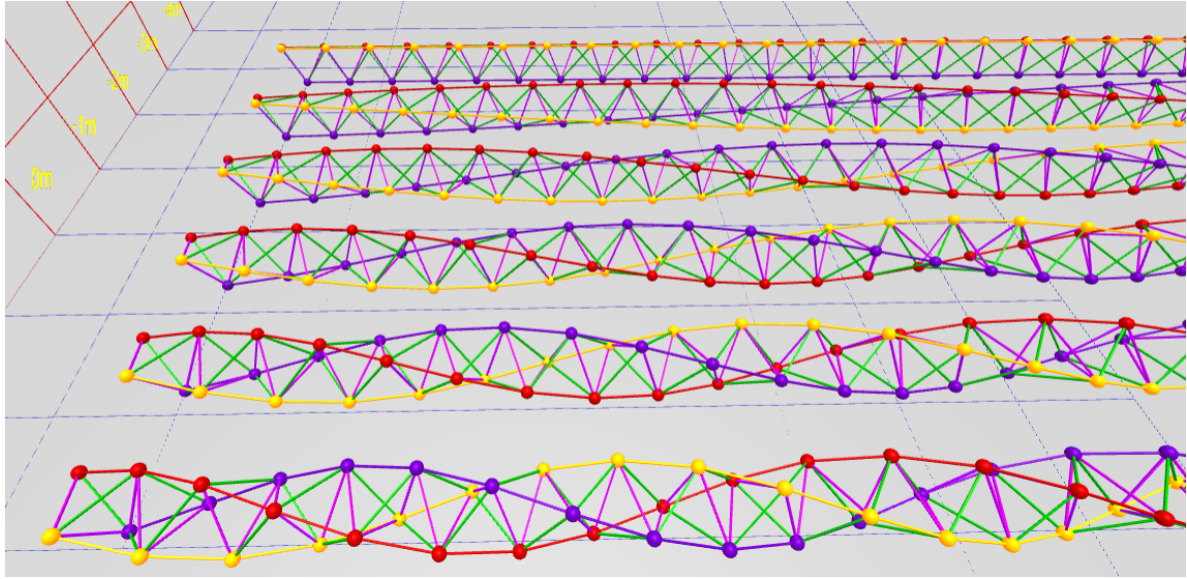


Figure 3. A Continuum of Tetrahelices

41 A BC helix does not rest stably on a plane. It is convenient to be able to “untwist” it and
 42 to form a tetrahelix space frame that has a flat planar surface. By making length changes in a
 43 certain way, we can untwist a tetrahelix to form a *tetrabeam* which has planar faces and has,
 44 for example, an equilateral triangular profile. This paper develops the equations needed to
 45 untwist the tetrahelix. All math developed here is available in JavaScript and demonstrated
 46 by an interactive design website <https://pubinv.github.io/tetrahelix/>[12], from which Figure 2
 47 and the figures below are taken.

48 Figure 3 displays a continuum of tetrahelices optimal in a certain sense, which is the result
 49 of this paper. The closest helix is the BC helix, and the furthest is the equitetrabeam, defined
 50 in section 6.

51 **2. A Designer’s Formulation of the BC Helix.** We would like to design nearly regular
 52 tetrahelices with a formula that gives the vertices in space. Eventually we would like to design
 53 nearly regular tetrahelices by choosing the lengths of a small set of members. In a space frame,
 54 this is a static design choice; in a tetrobot, it is a dynamic choice that can be used to twist
 55 the robot and/or exert linear or angular force on the environment.

56 Ideally we would have a simple formula for defining the nodes based on any curvature
 57 or pitch we choose. It is a goal of this paper to relate these two approaches to generating a
 58 tetrahelix continuum.

59 H.S.M Coxeter constructs the BC helix[3] as a repeated rotation and translation of the
 60 tetrahedra, showing the rotation is:

$$61 \quad \theta_{bc} = \arccos(-2/3)$$

62 and the translation:

63
$$h_{bc} = 1/\sqrt{10}$$

64 θ_{bc} is approximately $0.37 \cdot 2\pi$ radians or 131.81 degrees. The angle θ_{bc} is the rotation of
 65 each tetrahedron, not the tetrahedra along a rail. In [Figure 2](#), each tetrahedron has either a
 66 yellow, blue, or red outer edge or rail. That is, a blue-rail tetrahedron is rotated slightly more
 67 than a $1/3$ of a revolution to match the face of the yellow tetrahedra.

68 R.W. Gray's site[\[6\]](#), repeating a formula by Coxeter[\[3\]](#) in more accessible form, gives the

69 Cartesian coordinates $\begin{bmatrix} x \\ y \\ z \end{bmatrix}$ for a counter-clockwise BC Helix:

70 (1)
$$V(n) = \begin{bmatrix} r_{bc} \cos n\theta_{bc} \\ r_{bc} \sin n\theta_{bc} \\ nh_{bc} \end{bmatrix}, \text{ where: } \begin{aligned} r_{bc} &= \frac{3\sqrt{3}}{10} \approx 0.5196 \\ h_{bc} &= 1/\sqrt{10} \approx 0.3162 \\ \theta_{bc} &= \arccos(-2/3) \end{aligned}$$

71 where n represents each integer numbered node in succession on every colored rail.

72 The apparent rotation of a vertex an outer-edge, $V(n)$ relative from $V(n+3)$ for any
 73 integer n in (1), is $3\theta_{bc} - 2\pi$.

74 This formula defines a helix, but it is not any of the apparent helices, or *rail* helices, of the
 75 BC helix, but rather one that winds three times as rapidly through all nodes. To a designer of
 76 tetrahelices, it is more natural to think of the three helices which are visually apparent, that
 77 is, those three which are closely approximated by the outer edges or rails of the BC helix. We
 78 think of each of these three rails as being a different color: red, blue, or yellow. This situation
 79 is illustrated in [Figure 4](#), wherein the black helix represents that generated by (1), and the
 80 colored helices are generated by (2).

81 In order to develop the continuum of slightly irregular tetrahelices described in [section 7](#),
 82 we need a formula that gives us the nodes of just one rail helix, denoted by color c and integer
 83 node number n :

84
$$(\forall n \in \mathbb{Z}, \forall c \in \{0, 1, 2\} : H_{BCcolored}(n, c) = V(3n + c))$$

85 Such a helix can be written:

86 (2)
$$H_{BCcolored}(n, c) = \begin{bmatrix} r_{bc} \cos ((3\theta_{bc} - 2\pi)n + c\theta_{bc}) \\ r_{bc} \sin ((3\theta_{bc} - 2\pi)n + c\theta_{bc}) \\ 3h_{bc}(n + c/3) \end{bmatrix}, \text{ where } \begin{aligned} r_{bc} &= \frac{3\sqrt{3}}{10} \\ h_{bc} &= 1/\sqrt{10} \\ \theta_{bc} &= \arccos(-2/3) \end{aligned}$$

87 In this formula, integral values of n may be taken as a node number for one rail and
 88 used to compute its Cartesian coordinates. Allowing n to take non-integer values defines a
 89 continuous helix in space which is close to the segmented polyline of the outer tetrahedra
 90 edges, and equals them at integer values.

91 [Figure 4](#) illustrates this difference with a 7-tetrahedra BC helix, which is in fact the same
 92 geometry as the robot illustrated in [Figure 11](#). Although the nodes coincide, (1) evaluated
 93 at real values generates the black helix which runs through every node, and (2) defines the
 94 red, yellow, and blue helices. (In this figure these rail helices have been rendered at a slightly

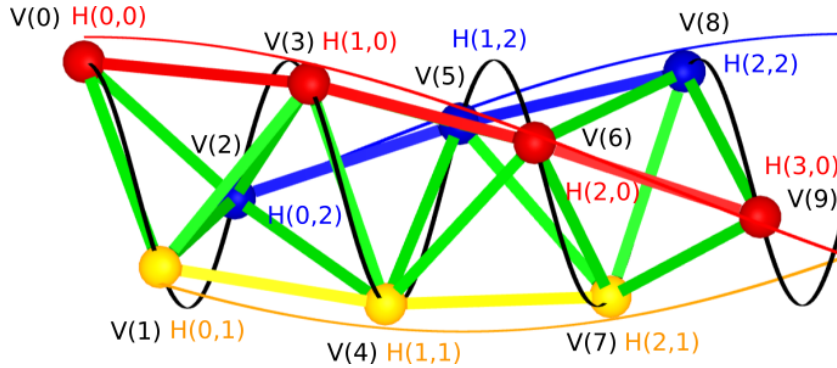


Figure 4. Rail helices (H) vs. Coxeter/Gray helix (V)

higher radius than the nodes for clarity; in actuality the maximum distance between the continuous, curved helix and the straight edges between nodes is much smaller than can be clearly rendered.)

The quantity $(3\theta_{bc} - 2\pi) \approx 35.43^\circ$ is the angular shift between $V(3n+c) = H_{BCcolored}(n, c)$ and $V(3(n+1)+c) = H_{BCcolored}(n+1, c)$. This quantity appears so often that we call it the “rail angle ρ ”. For the BC helix, $\rho_{bc} = (3\theta_{bc} - 2\pi)$.

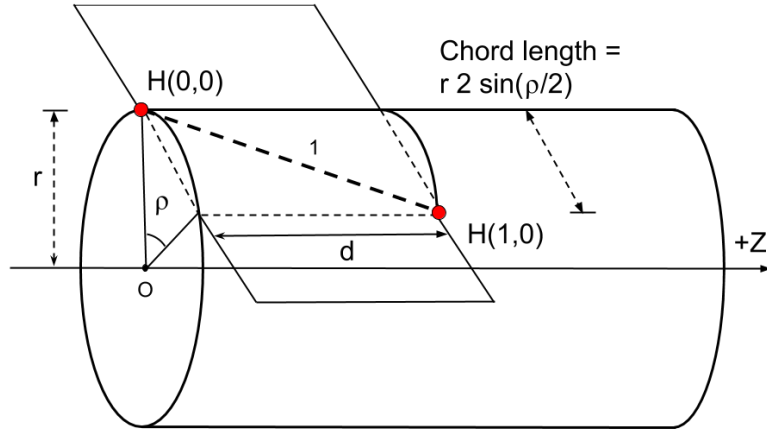


Figure 5. Rail Angle Geometry

Note in Figure 5 the z -axis travel for one rail edge is denoted by d . In (1) and (2), the variable h is used for one third of the distance we name d . We will later justify that $d = 3h$. In this paper we assume the length of a rail is always 1 as a simplification, except in proofs concerning rail length. (We make the rail length a parameter in our JavaScript code

105 in https://github.com/PubInv/tetrahelix/blob/master/js/tetrahelix_math.js [12].)

106 The $H_{BCcolored}(n, c)$ formulation can be further clarified by rewriting directly in terms of
107 the rail angle ρ_{bc} rather than θ_{bc} . Intuitively we seek an expression where $c/3$ is multiplied by
108 a $1/3$ rotation plus the rail angle ρ . We expand the expressions θ_{bc} and ρ_{bc} in (2) and seek to
109 isolate the term $c2\pi/3$.

$$\begin{aligned} 110 \quad c\theta_{bc} &= \{\text{we aim for } 3 \text{ in denominator, so we split...}\} \\ 111 \quad (c/3)(3\theta_{bc}) &= \{\text{we want } 2\pi \text{ in numerator, so add canceling terms...}\} \\ 112 \quad (c/3)((3\theta_{bc} - 2\pi) + 2\pi) &= \{\text{definition of } \rho_{bc}\}... \\ 113 \quad (c/3)\rho_{bc} + c2\pi/3 &= \{\text{algebra...}\} \\ 114 \quad c(\rho_{bc} + 2\pi)/3 & \\ 115 \end{aligned}$$

117 This allows us to redefine:

$$118 \quad (3) \quad H_{BCcolored}(n, c) = \begin{bmatrix} r \cos \rho_{bc} n + c(\rho_{bc} + 2\pi)/3 \\ r \sin \rho_{bc} n + c(\rho_{bc} + 2\pi)/3 \\ (n + c/3)h_{bc} \end{bmatrix}, \text{ where } \begin{aligned} \rho_{bc} &= (3\theta_{bc} - 2\pi) \\ h_{bc} &= 1/\sqrt{10} \end{aligned}$$

119 Recall that $c \in \{0, 1, 2\}$, but n is continuous (rational or real-valued.) We can now assert
120 that in Figure 4 the black helix winds at $\frac{3\theta_{bc}}{\rho_{bc}} \approx 11.16$ times the rate of a rail helix.

121 From this formulation it is easy to see that moving one vertex on a rail ($H_{BCcolored}(n, c)$)
122 to $H_{BCcolored}(n + 1, c)$ for any n and c) moves us ρ_{bc} radians around a circle. Since:

$$123 \quad \frac{2\pi}{\rho_{bc}} \approx 10.16$$

124 we can see that there are approximately 10.16 red, blue or yellow tetrahedra on one rail in a
125 single revolution.

126 The *pitch* of any tetrahelix, defined as the axial length of a complete revolution where
127 $\rho \neq 0$ is:

$$128 \quad (4) \quad p(\rho) = \frac{2\pi \cdot d}{\rho}$$

129 The pitch of the Boerdijk–Coxeter helix of edge length 1 is the length of three tetrahedra
130 times this number:

$$131 \quad \frac{3h_{bc} \cdot 2\pi}{\rho_{bc}} = \frac{6\pi}{\sqrt{10}\rho_{bc}} \quad \approx 9.64$$

133 The pitch is less than the number of tetrahedra because the tetrahedra are not lined
134 up perfectly. It is a famous and interesting result that the pitch is irrational. A BC helix
135 never has two tetrahedra at precisely the same orientation around the z -axis. However, this
136 is inconvenient to designers, who might prefer a rational pitch. The idea of developing a

137 rational period by arranging solid tetrahedra by relaxing the face-to-face matching has been
138 explored[13]. We develop below slightly irregular edge lengths that support, for example, a
139 pitch of precisely 12 tetrahedra in one revolution which would allow an architect to design a
140 column having a basis and a capital in the same relation to the tetrahedra they touch at the
141 bottom and top of the column.

142 **3. Optimal Tetrahelices are Triple Helices.** We use the term *tetrahelix* to mean any
143 structure made of vertices and edges which is isomorphic to the BC helix and in which the
144 vertices lie on three helices. We further demand that all edge lengths be finite, as we are only
145 interested in physically constructable tetrahelices. By isomorphic we mean there is a one-
146 to-one mapping between both vertices and edges in the two tetrahelices. One could consider
147 various definitions of optimality for a tetrahelix, but the most useful to us as robotocists
148 working with the Tetrobot concept is to minimize the maximum ratio between any two edge
149 lengths, because the Tetrobot uses mechanical linear actuators with limited range of extension.

150 A *triple helix* is three congruent helices that share an axis. We show that optimal tetra-
151 helices are in fact triple helices with the same radius, so that all vertices are on a cylinder.
152 In, stages, we demonstrate that optimal tetrahelices:

- 153 1. have the same pitch,
- 154 2. have parallel axes,
- 155 3. share the same axis,
- 156 4. have the same radius,
- 157 5. have the same rail lengths,
- 158 6. have axially equidistant nodes, and therefore
- 159 7. are in fact triple helices.

160 Suppose that all three rails do not have the same pitch. Starting at any shortest edge
161 between two rails, as we move from node to node away from our start edge the edge lengths
162 between rails must always lengthen without bound, which cannot be optimal. So we are
163 justified in talking about the *pitch* of the optimal tetrahelix as the pitch of its three rail
164 helices, even though there are three such helices of equivalent pitch.

165 Similarly, if the axes are not parallel, there is an edge of unbounded length in the structure,
166 so we do not consider such cases.

167 Define a *minimax edge-length optimal tetrahelix* or just an *optimal tetrahelix* to be a
168 tetrahelix for which there exists no other tetrahelix with lower ratio of longest edge length to
169 shortest edge length.

170 We wish to show that in an optimal tetrahelix, all vertices lie on the cylinder of radius r ,
171 regardless of where they lie on the z -axis.

172 As a little lemma for the proof below, observe that a tetrahelix of zero radius, where all
173 points lie on the same line, is not as optimal as a tetrahelix of a small radius. The edges
174 between rails will be shorter than the rail edges, and moving them apart slightly lengthens
175 the between-edge rails.

176 **Theorem 1.** *Any optimal tetrahelix with a rail angle of magnitude less than π has all three
177 axes coincident.*

178 *Proof.* Case 1: Suppose that ρ is zero. Then for any given inradius, the figure in the

179 XY -plane of an equilateral triangle is the minimax solution for all non-rail edges. Since all
 180 rail edges are of length 1, this is the minimax solution for the entire set. Since the vertices of
 181 an equilateral triangle lie on a circle, all points in three-space lie on a cylinder.

182 Case 2: Suppose that ρ is positive but less than π . In this case each rail helix has
 183 curvature. The projection of points in the XY plane creates a figure guaranteed to have
 184 point on either side of any line through the axis of such a helix, because the figure is either
 185 an n -gon or a circle. We show that the three helices share a common axis.

186 Without loss of generality define the Red helix to have its axis on the z -axis. Without
 187 loss of generativity define the Blue helix to be a helix that has an edge connection to the Red
 188 helix that is either a maximum or a minimum. Let B' be the blue helix translated in the
 189 XY -plane so that its axis is the z -axis and condicent with the red helix R . Let D be the
 190 distance between the axis of the Blue helix B and B' . We will show that if $D > 0$ then B
 191 “wobbles” in a way that cannot be optimal. Define a wobble vector by:

$$192 \quad W(n) = B(n) - B'(n)$$

193 where $B(n)$ is the cartesian vector $\begin{bmatrix} x \\ y \end{bmatrix}$ for the projection of the n th blue vertex. Note that
 194 $\|R(n) - B'(n+k)\|$ is a constant for any k , because R and B' have the same pitch and the
 195 same axis, even if they do not have the same radius (which we are currently proving.)

196 [Figure 6](#) demonstrates illustrates this situation. Like most diagrams, it is over specific,
 197 in that the two circles are drawn of the same radius but we do not depend upon that in this
 198 proof. The diagram represents the projection along the z axis of points into the XY -plane.

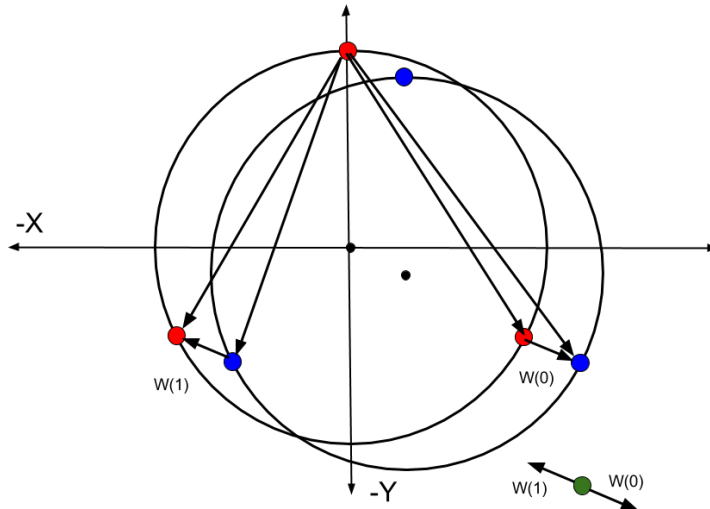


Figure 6. Wobble Vectors from Non-Coincident Axes

199 Since $-\pi < \rho < \pi$, each rail helix rotates about its axis as a function of n and defines at

200 least 3 unique points when projected onto the XY -plane around its axis. If $2\pi/\rho$ is irrational,
 201 it defines a circle. If $2\pi/\rho$ is rational it defines an n -gon in the XY -plane, where n is at least
 202 3 (when $\rho = 2\pi/3$). The set of wobbles $\{W(n)|\text{for any } n\}$ thus contains at least three vectors,
 203 pointing in different directions. For any point not at the origin, at least one of these vectors
 204 moves closer to the point and at least one moves further away.

205 The set of all lengths in the tetrahelix is a superset of: $L = \{\|R(n) - B(n)\|\}$, which by
 206 our choice has at least one longest or shortest length. $L = \{\|R(n) - (B'(n) + W(n))\|\}$ and
 207 so $L = \{\|(R(n) - B'(n)) - W(n)\|\}$. But $R(n) - B'(n)$ is a constant, so the minimax value of
 208 L is improved as $\|W(n)\|$ decreases. By our choice, this improves the minimax value of the
 209 total tetrahelix.

210 This process can be carried out on both the Blue and Yellow helices (perhaps simulta-
 211 neously) until $W(n)$ is zero for both, finding a tetrahelix of improved overall minimax value
 212 at each step. So a tetrahelix is optimal only when $W(n) = 0$, and therefore when $D = 0$
 213 $B(n) = B'(n)$, all three axes are conincident. ■

214 Now that we have show that axes are conincident and parallel and that the pitches are
 215 the same for all helices, we can assert that any optimum tetrahelix can be generated with an
 216 equation for helices:

217 (5)
$$V_{\text{triple}}(n, c) = \begin{bmatrix} r_c \cos(n\alpha + c2\pi/3 + \phi_c) \\ r_c \sin(n\alpha + c2\pi/3 + \phi_c) \\ \frac{d(n+c/3)}{3} \end{bmatrix}, \text{where: } c \in \{0, 1, 2\}$$

218 which would not be much more complicated if the axes where not coincident. Note that we
 219 have not yet show that the relationships of the radius r or the phase ϕ for the three helies, so
 220 we denoted them with a c subscript to show they are dependent on the color. In section 4 we
 221 give a more specific version of this formula which is optimal.

222 In principle in any three helices generated with (5) has at most nine distinct edge length
 223 classes. Each edge that connects two rails potentially has a longer length and shorter length
 224 we denote with a $+$ or $-$. So the classes are $\{RR, BB, YY, RB_+, RB_-, BY_+, BY_-, RY_+, RY_-\}$.
 225 If when projecting all vertices onto (dropping the x and y coordinates) the z -axis, the interval
 226 defined by the z axis value of its endpoints contains no other vertices, we call it a *one-hop*
 227 edge, and if it does contain another vertex we call it a *two-hop* edge. Then there are 3 rail
 228 edges $\{RR, BB, YY\}$, 3 one-hop lengths $\{RB_-, BY_-, RY_-\}$ between each pair of 3 rails, and
 229 3 two-hop lengths $\{RB_+, BY_+, RY_+\}$ between each pair of 3 rails, where the two-hop length
 230 is at least the one-hop length. However, if we generate the three helices symmetrically with
 231 (5), many of these lengths will be the same. In fact, it is possible that there will be only two
 232 distinct such classes.

233 Now we show that an optimal tetrahelix has the same radii for all three helices. To do this
 234 exhibit a symmetric tetrahelix (not yet shown to be optimal) which happens to be a triple
 235 helix, that has the property that all rail edges are equal to all one-hop edges and all two-hop
 236 edges are equal. Observe that although we have not get given the formula for the radii of
 237 such a triple helix, we observe there are some values for r and α , and ϕ for which all the three
 238 helices are symmetrically and evenly spaced. Furthermore, we can choose these values such
 239 that the three rail edges are of length unity and so that the one-hop lengths are also all of

length unity, and the two-hop lengths are slightly longer. We call such a tetrahelix a two-class tetrahelix.

Now consider a tetrahelix in which the radius of one of the helices is different. By the connections made in a tetrahelix, any increase to a radius increases both a one-hop and two-hop distance, and any decrease likewise decreases two. Since there exists a tetrahelix which has only two distinct classes of edge lengths, (the smaller being one-hop = rail, the larger being the two-hop distance), the helix with a larger radius increases a longest edge without increasing a shortest edges. Likewise, a helix with a smaller radius decreases a one-hop edge without decreasing a two-hop edge. Therefore, a tetrahelix with different radii is not optimal as some two-class tetrahelix generated by (5), and so it not optimal. We have not yet proved that a two-class tetrahelix is optimal, but it suffices to show that there exist such a better tetrahelix to show that different radii imply a suboptimal tetrahelix.

Because an optimal tetrhelix has equivalent radii and equivalent pitch for all three helices, it has equivalent rail edge lengths. Likewise, there is a single rail angle ρ that represents the rotation of two nodes connected by a single rail edge, and it is the same for all three rails.

Now that we have shown that any optimal tetrahelix vertices are on helices of the same axes and pitch, we see that the vertices of any optimal tetrahelix will lie on a cylinder, or a circle when axis dimension is projected out. Therefore it is reasonable to now speak of the singular *radius* r of a tetrahelix as the radius of the cylinder. We can now go on to the harder proof about where vertices occur along the z -axis.

We show that in fact the nodes must be distributed in even thirds along the z -axis, as in fact they are in the regular BC helix.

Note that from the point of view of a single edge, we are on a slanted cylinder, when $\rho \neq 0$. This means from its point of view a cross section is an ellipse. So we have to be very careful in comparing lengths of edges relative to the tetrahedron, because a change in position along the edge changes the length of a line, but in a complicated way depending on where it is relative to the ellipse.

However, we have already shown the rail lengths are equal in any optimal tetrahelix.

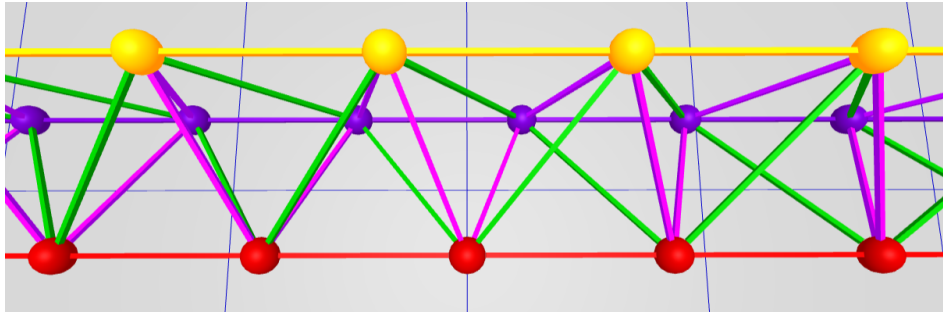


Figure 7. Equitetrabeam

Figure 7 shows the equitetrabeam, which is defined in section 6, but also conveniently illustrates the one-hop and two-hop edge definitions. The green edges are the two-hop edges and the purple edges are the one-hop edges. Note that the green edges are slightly longer than the purple edges.

272 **Theorem 2.** *An optimal tetrahelix of any rail angle $\rho < \pi$ is a triple helix with all vertices
273 evenly spaced at $d/3$ intervals on the z axis. Any one tetrahedron in a tetrahelix has 1 rail
274 edge, 2 one-hop edges connected to the rail and 2 two-hop edges connected to the rail. The
275 edge opposite of the rail edge is a one-hop edge.*

276 **Proof.** Consider the tetrahelix in which the vertices are evenly spaced at $d/3$ intervals on
277 the z axis. Every edge is either a rail edge, or it makes one hop, or it makes two hops. All of
278 the one-hop edges are equal length. All of the two-hop edges are equal length.

279 Every vertex is connected to 4 non-rail edges. There is a one-hop edge in both the positive
280 and negative z direction. Likewise there is a two-hop edge in both the positive and negative
281 z direction. Let A be the set of edge lengths, which has only 3 members, represented by
282 $A = \{o, t, r\}$ for the one-hop, two-hop, and rail edge lengths.

283 Any attempt to move any rail in either z direction lengthens one two-hop edge to t' , where
284 $t' > t$ and shortens one one-hop edge $o' < o$. Let $B = \{o', t'\} \cup A$ be new edges. The minimax
285 of B is greater than the minimax of A since there is a single rail length which cannot be both
286 greater than t' and o' and less than t' and o' . Therefore, any optimal tetrahelix has all one-hop
287 edges between all rails equal to each other, and all two-hop edges equal to each other, and the
288 z distances between rails equal, and therefore $d/3$ from each other.

289 Note that based on [Theorem 2](#), there are only 3 possible lengths in an optimal tethrahelix,
290 and we are justified in classifying edge lengths as *rail*, *one-hop*, or *two-hop*. The one-hop edges
291 are the edges between rails that are closest on the z -axis, and the two-hop edges are those
292 that skip over a vertex.

293 In [section 4](#) have not yet investigated in the general case the relationships between α ,
294 r , ϕ and d in [\(5\)](#). However, we observe that when $\alpha = 0$, the helices are degenerate, having
295 curvature of 0, and we have the equitetrabeam.

296 Taking all of these results together, each helix in an optimal tetrahelix is congruent to the
297 others, shares an axis, is the same radius, and are evenly spaced axially. An optimal tetrahelix
298 is therefore a *triple helix*.

299 **4. Parameterizing Tetrahelices via Rail Angle.** We seek a formula to generate optimal
300 tetrahelices that accepts a parameter that allows us to design the tetrahelix conveniently.
301 Please refer back to [Figure 5](#). The pitch of the helix is an obvious choice, but is not defined
302 when the curvature is 0, an important special case. The radius or the axial distance between
303 two nodes on the same rail are possible choices, but perhaps the clearest choice is to build
304 formulae that takes as their input the “rail angle” ρ . We define ρ to be the angle formed in
305 the X,Y plane $\angle H(0,0)OH(0,1)$ projecting out the z axis and sighting along the positive z
306 axis. In other words, ρ controls how far a rail edge of a tetrahelix deviates from being parallel
307 with the axis, or the “twistiness” of the tetrahelix. We use the parameter $\chi = 1$ to indicate a
308 chirality of counter-clockwise, and $\chi = -1$ for clockwise.

309 The quantities ρ, r, d are related by the expression:

$$\begin{aligned} 310 \quad & 1^2 = d^2 + (2r \sin \rho/2)^2 \\ 311 \quad (6) \quad & d^2 = 1 - 4r^2(\sin \rho/2)^2 \\ 312 \quad & \end{aligned}$$

314 Checking the important special case of the BC helix, we find that this equation indeed
 315 holds true (treating d in this equation as $3h_{bc}$ as defined by Gray and Coxeter, that is,
 316 $d_{bc} = 3h_{bc}$, where they are using h for the axial height from one node to the next of a different
 317 color, but we use d to mean distance between nodes of the same color).

318 The rail angle ρ also has the meaning that $2\pi/\rho$ is the number of tetraheda in a full
 319 revolution of the helix.

In choosing ρ , one greatly constrains r and d , but does not completely determine both of them together, so we treat both as parameters.

322 Rewriting our formulation in terms of ρ :

$$H_{general}(\chi, n, c, \rho, d_\rho, r_\rho) = \begin{bmatrix} r_\rho \cos(\chi \cdot (n\rho + c(\rho + 2\pi)/3)) \\ r_\rho \sin(\chi \cdot (n\rho + c(\rho + 2\pi)/3)) \\ d_\rho(n + c/3) \end{bmatrix}$$

where: $1 = d_\rho^2 + 4r_\rho^2(\sin \rho/2)^2$
 $\chi \in \{-1, 1\}$

H_{general} forces the user to select three values: ρ , r_ρ , and d_ρ satisfying (6). Note that when $\rho = 0$ then $d_\rho = 1$, but r_ρ is not determined by (6).

Theorem 3. The tetrahelices generated by H_{general} are optimal in terms of minimum maximum ratio of member length when r_ρ is chosen so that the length of the one-hop edge is equal to the rail length.

331 *Proof.* This is proved by a minimax argument.

By [Theorem 2](#), we can compute the (at most) three edge-lengths of an optimal tetrahelix by formula universally quantified by n and c :

rail = $dist(H_{general}(n, c, \rho, d_\rho, r_\rho), H_{general}(n + 1, c, \rho, d_\rho, r_\rho)) = 1$
 one-hop = $dist(H_{general}(n, c, \rho, d_\rho, r_\rho), H_{general}(n, c + 1, \rho, d_\rho, r_\rho))$
 two-hop = $dist(H_{general}(n, c, \rho, d_\rho, r_\rho), H_{general}(n, c + 2, \rho, d_\rho, r_\rho))$

339 where $dist$ is the Cartesian distance function.

340 one-hop = $dist(H_{general}(n, c, \rho, d_\rho), H_{general}(n, c + 1, \rho, d_\rho), r_\rho)$

341 one-hop = $\sqrt{\frac{d_\rho^2}{9} + r_\rho^2(\sin^2(\rho/3 + \frac{2\pi}{3}) + (1 - \cos(\rho/3 + \frac{2\pi}{3}))^2)}$

342 but: $d_\rho^2 = 1 - 4r_\rho^2(\sin(\rho/2)^2)$...so we substitute:

343 one-hop = $\sqrt{\frac{1}{9} + r_\rho^2(-\frac{4(\sin^2(\rho/2))}{9} + \sin^2(\rho/3 + \frac{2\pi}{3}) + (1 - \cos(\rho/3 + \frac{2\pi}{3}))^2)}$

344

346 By similar algebra and trigonometry:

347 two-hop = $\sqrt{\frac{4}{9} + r_\rho^2(-\frac{16(\sin^2(\rho/2))}{9} + \sin^2(2\rho/3 + \frac{4\pi}{3}) + (1 - \cos(2\rho/3 + \frac{4\pi}{3}))^2)}$

348

350 By definition of minimax edge length optimality, we are trying to minimize:

351
$$\frac{\max \{1, \text{one-hop}(r), \text{two-hop}(r)\}}{\min \{1, \text{one-hop}(r), \text{two-hop}(r)\}}$$

352 But since $\text{two-hop}(r) \geq \text{one-hop}(r)$, this is equivalent to:

353
$$\frac{\max \{1, \text{two-hop}(r)\}}{\min \{1, \text{one-hop}(r)\}}$$

354 This quantity will be equal to one of:

355
$$\frac{\text{two-hop}(r)}{1}, \frac{1}{\text{one-hop}(r)}, \frac{\text{two-hop}(r)}{\text{one-hop}(r)}$$

356 We know that both $\text{one-hop}(r)$ and $\text{two-hop}(r)$ increase monotonically and continuously
357 with increasing r . By inspection it seems likely that we will minimize this set by equating
358 $\text{one-hop}(r)$ or $\text{two-hop}(r)$ to 1, but to be absolutely sure we must examine the partial derivative
359 of the ratio $\frac{\text{two-hop}(r)}{\text{one-hop}(r)}$ in this range.

360 Although complicated, we can use Mathematica to investigate the partial derivative of the
361 $\text{two-hop}(r) - \text{one-hop}(r)$ with respect to the radius to be able to understand how to choose
362 the radius to form the minimax optimum.

363 Let:

364
$$f_\rho = -\frac{4(\sin^2(\rho/2))}{9}$$

365

366
$$g_\rho = -\frac{16(\sin^2(\rho/2))}{9}$$

367 $j_\rho = \sin^2(\rho/3 + \frac{2\pi}{3}) + (1 - \cos(\rho/3 + \frac{2\pi}{3}))^2)$

368
369 $k_\rho = (\sin^2(2\rho/3 + \frac{4\pi}{3}) + (1 - \cos(2\rho/3 + \frac{4\pi}{3}))^2)$

370 Then:

371 $\frac{\text{two-hop}}{\text{one-hop}} = \frac{\sqrt{\frac{4}{9} + r_\rho^2(g_\rho + j_\rho)}}{\sqrt{\frac{1}{9} + r_\rho^2(f_\rho + k_\rho)}}$

373 By graph inspection using Mathematica, we see the partial derivative of this with respect
374 to radius r_ρ is always negative. Since the partial derivative of two-hop/one-hop with respect
375 to the radius r_ρ is negative up until ρ_{bc} , this ratio goes down as the radius goes up, and we
376 optimize the overall minimax distance by choosing the largest radius up until one-hop = 1,
377 the rail-edge length.

378 Therefore we decrease the minimax length of the whole system as we increase the radius
379 up to the point that the shorter, one-hop distance is equal to the rail-length, 1. Therefore, to
380 optimize the whole system so long as $\rho \leq \rho_{bc}$, we equate one-hop to 1 to find the optimum
381 radius:

382 $1 = \sqrt{\frac{1}{9} + r_{opt}^2(-\frac{4(\sin^2(\rho/2))}{9} + \sin^2(\rho/3 + \frac{2\pi}{3}) + (1 - \cos(\rho/3 + \frac{2\pi}{3}))^2)}$
383 (8) $r_{opt} = \frac{2}{\sqrt{\frac{9}{2} \cdot (\sqrt{3}\sin(\rho/3) + \cos(\rho/3)) + \cos(\rho) + 8}}$

384

386 We can now give a formula for d_{opt} computed from ρ, r_{opt} via the rail angle equation (6):

387 $d_{opt}^2 = 1 - 4\left(\frac{2}{\sqrt{\frac{9}{2} \cdot (\sqrt{3}\sin(\rho/3) + \cos(\rho/3)) + \cos(\rho) + 8}}\right)^2(\sin(\rho/2))^2$
388 $d_{opt}^2 = 1 - \frac{16(\sin(\rho/2))^2}{9(\sqrt{3}\sin(\rho/3) + \cos(\rho/3)) + \cos(\rho) + 8}$
389 (9) $d_{opt} = \sqrt{1 - \frac{16\sin^2(\rho/2)}{\cos(\rho) + 9(\sqrt{3}\sin(\rho/3) + \cos(\rho/3)) + 8}}$

390

392 Thus, by computing r_{opt} and d_{opt} as a function of ρ from this equation, we can construct
393 minimax optimal tetrahelix for an $0 \leq \rho \leq \rho_{bc}$. ■

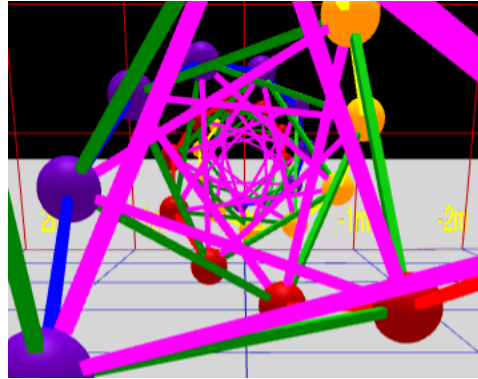


Figure 8. Axial view of a BC-Helix

5. The Inradius. Since the axes are parallel, we may define the *inradius*, represented by the letter i , of a tetrahelix to be the radius of the largest cylinder parallel to this axis that is surrounded by each tetrahelix and pentrated by no edge.

If we look down the axis of an optimal tetrahelix as shown in Figure 8, it happens that only the one-hop edges (rendered in purple in our software) comes closest to the axis. In other words, they define the radius of the incircle of the projection, or the radius of a cylinder that would just fit inside the tetrahelix. A formula for the inradius of the tetrahelix is useful if you are designing it as a structure that bears something internally, such as a firehose, a pipe, or a ladder for a human. The inradius $r_{in}(\rho)$ of an optimal tetrahelix is a remarkably simple function of the radius r and the rail angle ρ :

$$404 \quad (10) \qquad r_{in}(\rho) = r \sin \frac{\pi - \rho}{6}$$

405 Which can be seen from the trigonometry of a diagram of the projected one-hop edges con-
406 necting four sequentially numbered vertices:

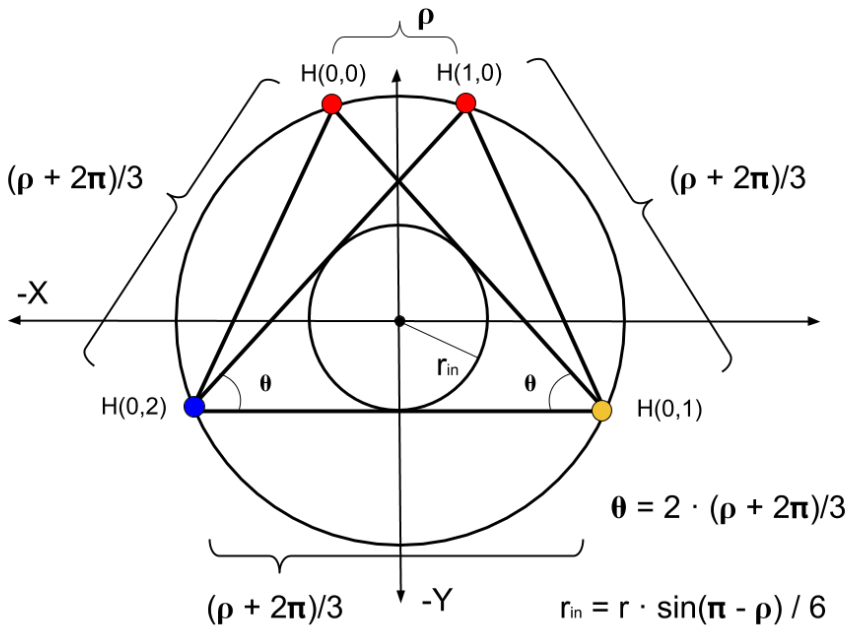


Figure 9. General One-hop Projection Diagram

407 From this equation with the help of symbolic computation we observe that inradius of the
 408 BC helix of unit rail length is $r_{in}(\rho_{bc}) = \frac{3}{10\sqrt{2}} \approx 0.21$.

409 **6. The Equitetrabeam.** Just as $H_{general}$ constructs the BC helix (with careful and non-
 410 obvious choices of parameters) which is an important special case due to its regularity, it
 411 constructs an additional special (degenerate) case when the rail angle $\rho = 0$ and $d = 1$ (the
 412 edgelength), where the cross sectional area is an equilateral triangle of unchanging orientation,
 413 as shown in Figure 7 and at the rear of Figure 3. We call this the *equitetrabeam*. It is not
 414 possible to generate an equitetrabeam from (1) without the split into three rails introduced
 415 by (2) and completed in (7).

416 **Corollary 4.** *The equitetrabeam with minimal maximal edge ratio is produced
 417 by $H_{general}$ when $r = \sqrt{\frac{8}{27}}$.*

418 **Proof.** Choosing $d = 1$ and $\rho = 0$ we use Equation (8) to find the radius of optimal
 419 minimax difference.

420 Substituting into (7):

$$\text{one-hop} = \sqrt{\frac{1}{9} + 3r^2}$$

422

424 Then:

425
$$1 = \sqrt{\frac{1}{9} + 3r^2}$$
 solved by...

426
$$r = \sqrt{\frac{8}{27}}$$
 ≈ 0.54

427

■

429 This radius¹ produces a two-hop rail length of $\frac{2}{\sqrt{3}}$. The difference between this and 1 is
430 $\approx 15.47\%$. The inradius of the equitetrabeam of unit rail length from both Equation (10) and
431 the fact that the inradius of an equilateral triangle is half the circumradius is $\sqrt{\frac{8}{27}}/2$, or $\frac{\sqrt{6}}{9}$.

432 In Figure 3, the furthest tetrahelix is the optimal equitetrabeam. Figure 7 is a closeup of
433 an equitetrabeam.

434 To the extent that we value tetrabeams (that is, tetrahelices with a rail angle of 0, and
435 therefore zero curvature and curvature) as mathematical or engineering objects, we have
436 motivated the development of $H_{general}$ as a transformation of $V(n)$ defined by Equation (1)
437 from Gray and Coxeter. It is difficult to see how the $V(n)$ formulation could ever give rise
438 to a continuum producing the tetrabeam, since setting the angle in that equation to zero can
439 produce only collinear points.

440 The equitetrabeam may possibly be a novel construction. The fact that 6 members meet
441 in a single point would have been a manufacturing disadvantage that may have dissuaded
442 structural engineers from using this geometry. However, the advent of additive manufacturing,
443 such a 3D printing, and the invention of two distinct concentric multimember joints[15, 7] has
444 improved that situation.

445 Note that the equitetrabeam has chirality, which becomes important in our attempt to
446 build a continuum of tetrahelices.

447 **7. An Untwisted Continuum.** We observe that Equations (8) and (9) compute r_{opt} and
448 d_{opt} which create an optimal tetrahelix for any rail angle ρ between 0, which gives the equi-
449 tetrabeam and $\rho_{bc} \approx 35.43^\circ$, which gives the BC helix.

450 Because the equitetrabeam which has a rail angle of 0 still has chirality, that is, one still
451 must decide to connect the one-hop edge to the clockwise or the counter-clockwise node, it
452 is not possible to build a smooth continuum where ρ transitions from positive to negative
453 which remains optimal. One can use a negative ρ in $H_{general}$ but it does not produce minimax
454 optimal tetrahelices. In other words, untwisting a counter-clockwise tetrahelix to rail angle 0
455 and then going even further does produce a clockwise tetrahelix, but one in which the one-hop
456 and two-hop lengths in the wrong places (that is, two-hop becomes shorter than one-hop.)
457 Likewise, $\rho > \rho_{bc}$ generates a tetrahelix, but minimax optimality is not guaranteed by $H_{general}$.

458 The pitch of a helix (see (4), for a fixed z -axis travel d , is trivial. However, if one is
459 computing z -axis travel from (9) the pitch is not simple. It increases monotonically and
460 smoothly with decreasing ρ , so Equation (4) can be easily solved numerically with a Newton-

¹Another interesting but non-optimal solution is derived by setting $(\text{one-hop} + \text{two-hop})/2 = 1$, occurs at $r = \sqrt{35}/4$ which produces three length classes of $11/12, 12/12, 13/12$.

461 Raphson solver, as we do on our website. For a pitch at least $p \geq \frac{3\sqrt{2}\pi}{\sqrt{5}\rho_{bc}} \approx 9.64$, using (9)
462 produces minimax optimal tetrahelices.

463 In this way a rail angle can be chosen for any desired (sufficiently large) pitch, yield the
464 optimum radius, one-hop, and two-hop lengths an engineer needs to construct a physical
465 structure.

466 The curvature of a rail helix is formally given by:

467 (11)
$$\frac{|r_\rho|}{r_\rho^2 + (d_\rho/\rho)^2}$$

468 which goes to 0 as ρ approaches 0 (the equitetrabeam.) As ρ increase up to ρ_{bc} the curvature
469 increases smoothly until the BC Helix is reached.

470 Perhaps surprisingly, the optimal untwisting is accomplished only by changing the length
471 of the two-hop member, leaving the one-hop member and rail length equivalent within this
472 continuum.² However, it should be noted that an engineer or architect may also use $H_{general}$
473 directly and interactively, and that minimax length optimality is a mathematical starting point
474 rather than the final word on the beauty and utility of physical structures. For example, a
475 structural engineer might increase radius past optimality in order to resist buckling.

476 If an equitetrabeam were actually used as a beam, an engineer might start with the
477 optimal tetrabeam and dilate it in one dimension to “deepen” the beam. Similarly, simple
478 length changes curve the equitetrabeam into an “arch”. The “colored” approach of (7) exposes
479 these possibilities more than the approach of (1).

480 Trusses and space frames remain an important design field in mechanical and structural
481 engineering[10], including deployable and moving trusses[2].

482 **8. Utility for Robotics.** Starting twenty years ago, Sanderson[14], Hamlin,[8], Lee[9], and
483 others created a style of robotics based on changing the lengths of members joined at the
484 center of a joint, thereby creating a connection to pure geometry. More recently NASA has
485 experimented with tensegrities[1], a different point in the same design spectrum. These fields
486 create a need to explore the notion of geometries changing over time, not generally considered
487 directly by pure geometry.

488 As suggested by Buckminster Fuller, the most convenient geometries to consider are those
489 that have regular member lengths, in order to facilitate the inexpensive manufacture and
490 construction of the robot. In a plane, the octet truss[4] is such a geometry, but in a line, the
491 Boerdijk–Coxeter helix is a regular structure.

492 However, a robot must move, and so it is interesting to consider the transmutations of
493 these geometries, which was in fact the motivation for creating the equitetrabeam.

494 **Theorem 5.** *By changing only the length of the longer members that connect two distinct
495 rails (the two-hop members), we can dynamically untwist a tetrobot forming the Boerdijk–
496 Coxeter configuration into the equitetrabeam which rests flat on the plane.*

²Before deriving Equation (8), we created a continuum by using a linear interpolation between the optimal radius for the Equitetrabeam and the BC Helix. This minimax optimum of this simpler approach was at most 1% worse than the optimum computed by (8).

497 *Proof.* Proof by our computer program that does this using Equation (7) applied to the
498 7-tet Tetrobot/Glussbot.

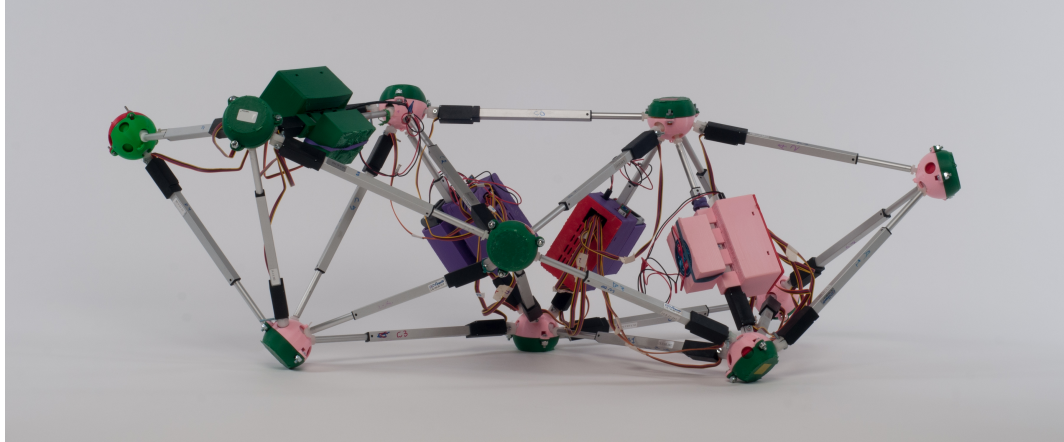


Figure 10. *Glussbot in relaxed, or BC helix configuration*

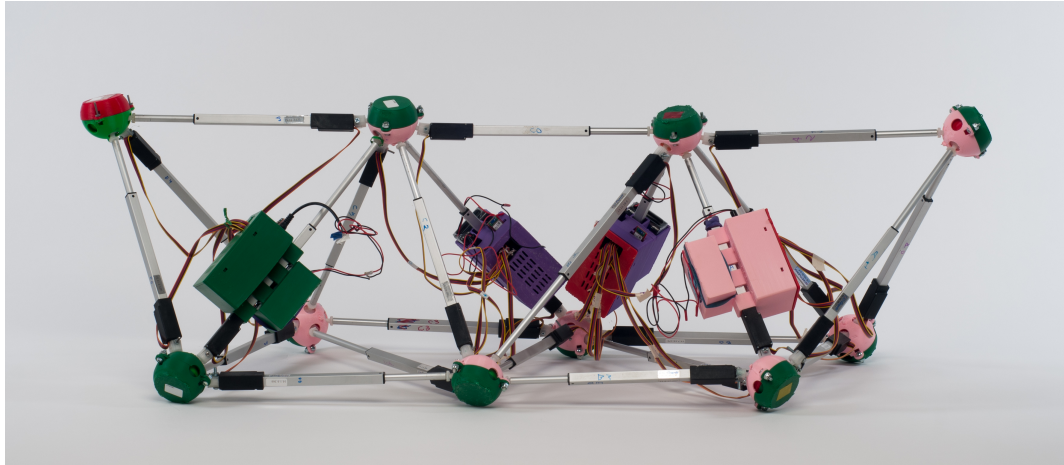


Figure 11. *The Equitetrabream: Fully Untwisted Glussbot in Hexapod Configuration*

499 By untwisting the tetrahelix so that it has a planar surface resting on the ground, we may
500 consider each vertex touching the ground a foot or pseudopod. A robot can thus become a
501 hexapod or n -pod robot, and the already well-developed approaches to hexapod gaits may be
502 applied to make the robot walk or crawl.

503 **9. Conclusion.** The BC Helix is the end point of a continuum of tetrahelices, the other end
504 point being an untwisted tetrahelix with equilateral cross section, constructed by changing the
505 length of only those members crossing the outside rails after hopping over the nearest vertex.
506 Under the condition of minimum maximum length ratios of all members in the system, all
507 such tetrahelices have vertices evenly spaced along the axis generated by a simple equation
508 and are in fact triple helices. A machine, such as a robot or a variable-geometry truss, that
509 can change the length of its members can thus twist and untwist itself by changing the length

510 of the appropriate members to achieve any point in the continuum. With a numeric solution,
511 a design may choose a rotation angle and member lengths to obtain a desired pitch.

512 **10. Contact and Getting Involved.** The Gluss Project <http://pubinv.github.io/gluss/> is
513 part of Public Invention <https://pubinv.github.io/PubInv/>, a free-libre, open-source research,
514 hardware, and software project that welcomes volunteers. It is our goal to organize projects for
515 the benefit of all humanity without seeking profit or intellectual property. To assist, contact
516 read.robert@gmail.com.

517

REFERENCES

- 518 [1] *NTRT - NASA Tensegrity Robotics Toolkit.* <https://ti.arc.nasa.gov/tech/asr/intelligent-robotics/tensegrity/ntrt/>. Accessed: 2016-09-13.
519
- 520 [2] J. CLAYPOOL, *Readily configured and reconfigured structural trusses based on tetrahedrons as modules*,
521 Sept. 18 2012, <https://www.google.com/patents/US8266864>. US Patent 8,266,864.
522
- 523 [3] H. COXETER ET AL., *The simplicial helix and the equation $\tan(n \theta) = n \tan(\theta)$* , Canad. Math. Bull, 28
524 (1985), pp. 385–393.
525
- 526 [4] R. FULLER, *Synergetic building construction*, May 30 1961, <https://www.google.com/patents/US2986241>.
527 US Patent 2,986,241.
528
- 529 [5] R. FULLER AND E. APPLEWHITE, *Synergetics: explorations in the geometry of thinking*, Macmillan, 1982,
530 <https://books.google.com/books?id=G8baAAQMAAJ>.
531
- 532 [6] R. W. GRAY, *Tetrahelix data*. <http://www.rwgrayprojects.com/rbfnotes/helix/helix01.html>, <http://www.rwgrayprojects.com/rbfnotes/helix/helix01.html> (accessed Accessed: 2017-04-08).
533
- 534 [7] G. J. HAMLIN AND A. C. SANDERSON, *A novel concentric multilink spherical joint with parallel robotics*
535 *applications*, in Proceedings of the 1994 IEEE International Conference on Robotics and Automation,
536 May 1994, pp. 1267–1272 vol.2, <https://doi.org/10.1109/ROBOT.1994.351313>.
537
- 538 [8] G. J. HAMLIN AND A. C. SANDERSON, *Tetrobot: A Modular Approach to Reconfigurable Parallel*
539 *Robotics*, Springer Science & Business Media, 2013, <https://play.google.com/store/books/details?id=izrSBwAAQBAJ> (accessed 2017-04-08).
540
- 541 [9] W. H. LEE AND A. C. SANDERSON, *Dynamic rolling locomotion and control of modular robots*, IEEE
542 Transactions on robotics and automation, 18 (2002), pp. 32–41.
543
- 544 [10] M. MIKULAS AND R. CRAWFORD, *Sequentially deployable maneuverable tetrahedral beam*, Dec. 10 1985,
545 <https://www.google.com/patents/US4557097>. US Patent 4,557,097.
546
- 547 [11] R. L. READ, *Gluss = Slug + Truss*. Unpublished preprint, <https://github.com/PubInv/gluss/blob/gh-pages/doc/Gluss.pdf> (accessed 2016-10-27).
548
- 549 [12] R. L. READ, *Untwisting the tetrahelix website*. <https://pubinv.github.io/tetrahelix/>, <https://pubinv.github.io/tetrahelix/> (accessed 2017-04-08).
550
- 551 [13] G. SADLER, F. FANG, J. KOVACS, AND K. IRWIN, *Periodic modification of the Boerdijk-Coxeter helix*
552 *(tetrahelix)*, arXiv preprint arXiv:1302.1174, (2013), <https://arxiv.org/abs/1302.1174>.
553
- 554 [14] A. C. SANDERSON, *Modular robotics: Design and examples*, in Emerging Technologies and Factory Au-
555 tomation, 1996. EFTA'96. Proceedings., 1996 IEEE Conference on, vol. 2, IEEE, 1996, pp. 460–466.
556
- 557 [15] S. SONG, D. KWON, AND W. KIM, *Spherical joint for coupling three or more links together at one point*,
558 May 27 2003, <http://www.google.com/patents/US6568871>. US Patent 6,568,871.
559